Medium power laser versus electron beam interaction in graphite bulk target processing: A theoretical analysis

L. ȘUFARU[a, b], M. OANE[c], G. POPESCU-PELIN[b,c], N. MIHĂILESCU[c], A. BUCĂ[b], I. N. MIHĂILESCU[c,*]
[a]C.B.R.N. Defense and Ecology Scientific Research Center, 225 Olteniței Street, Bucharest, Romania
[b]Faculty of Physics, University of Bucharest, 405 Atomiștilor Street, Măgurele, Ilfov, Romania
[c]National Institute for Laser, Plasma and Radiation Physics, 409 Atomiștilor Street, Măgurele, Ilfov, Romania

We checked up the validity of the assumption that: the laser and electron beam processing have the same effects if one considers relatively high irradiation powers. The analysis was conducted in case of an incident power equal to 500W for either laser or electron beam. The simulations demonstrated that the assumption is valid with a high degree of precision.

1. Introduction

Laser and electron beam irradiation of solids recently focused much attention for various top scientific and technological applications [1-4]. Special emphases was put on the subsequent or synchronous action of the laser and electron beams in local transformation but also ablation and plasma production from various materials, in vacuum or controlled atmosphere (Sorescu M. 1995, Yang Z. 2013) [5, 6].

For an appropriate understanding of the involved phenomena and in order to ensure an optimum processing rate, one should be able to discriminate between the expected effects of the laser versus electron beams under similar irradiation conditions. Based upon these premises, correct experiments could be designed with the optimum energy transfer and processing rates by the two beams.

We herewith report on the results of a comparative study of medium power laser vs. electron beam irradiation of C, a material of key importance for many scientific and technological utilization.

2. Ablation mechanisms

As known, the Lambert Beer absorption law describing the laser-solid interaction reads as:

$$I_{mn}(x, y) = I_{0,mn} \cdot e^{-\alpha z} , \qquad (1)$$

where:

$$I_{mn}(x, y) = I_{\max, mn} \left[H_m(\tfrac{\sqrt{2}x}{w}) H_n(\tfrac{\sqrt{2}y}{w}) \times \exp\left[-\left(\tfrac{x^2+y^2}{w^2}\right)\right]\right]^2 . \qquad (2)$$

Here, I_{mn}, $I_{\max,mn}$, H_m, H_n stand for laser intensity in the mode {m,n}, maximum laser intensity in the mode {m,n} and the Hermite polynomial of order m and n, respectively. We are dealing with CO_2 lasers in cw mode and we take w=1mm.

One assumes that we are in the case: $m=0$ and $n=0$ in Eq 1.

For electron irradiation [7, 8], one should apply, in the particular case of graphite, the empirical absorption Katz and Penfolds law [7]. A Gaussian profile of the electron beam was considered.

We have chosen the total power of the laser and electron beams of 500 W [9].

The geometry of the simulation is depicted schematically in Fig. 1, where the electron beam propagates along the z axis and is incident on a graphite sample with dimensions of (4×4×15) mm³.
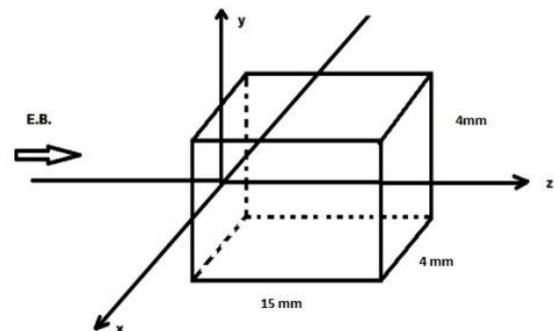

Fig. 1. Irradiation scheme of a small graphite sample

The geometry is in Cartesian coordinates and the transversal plane of the beam is the xy one. When calculating the stopping power three physical phenomena

should be taken into account: the secondary electron emission, the polarization of the target and the effect of magnetic field upon the incident beam.

For electrons with energies greater than 2.5 MeV their range in the target material is given by the formula put forward by Katz and Penfolds:

$$d_{max}[cm] = (0.530 \cdot E_{max}[MeV] - 0.106\,[cm])\,/\,\rho[g/cm^3].\quad (3)$$

E_{max} refers to the energy of the beam which determines the maximum range that the electrons of the beam can reach inside target. We further assume a linear dependency of the energy absorbed in the material with the distance z. The parameters defining this dependency can be found from the two boundary conditions at the incident surface where the beam hits the target and at d_{max}, where the beam deposits its energy. In our evaluation, we consider a graphite sample with ρ=2.23 g/cm^3 giving d_{max}=1.43 cm, inferior to the sample size. This leads to the following absorption law (in our case E_{max} =6.23MeV):

$$E_{abs}(z) = \begin{cases} 6.23 - 4.36 \cdot z, & for\, z \le d_{max} \\ 0, & for\, z > d_{max} \end{cases}.\quad (4)$$

Here, E_{abs} is in MeV and z is expressed in centimeters. Expression (4) is the source term for the heat equation as it will be shown in the next section.

3. Heat equation

Describing the thermal field during electron beam irradiation is not a new issue [7, 8, 10]. One thus has:

$$\frac{\partial^2 T}{\partial x^2} + \frac{\partial^2 T}{\partial y^2} + \frac{\partial^2 T}{\partial z^2} - \frac{1}{\gamma}\frac{\partial T}{\partial t} = -\frac{A(x,y,z,T)}{k}.\quad (5)$$

Here, T stands for the temperature variation relative to the initial value, T_0 that occurs by exposure to irradiation, A is the energy deposited by electrons per volume and time units, k and γ are the thermal conductivity and diffusivity of the sample. We have $A(x, y, z, t) = E_{abs}(z)/(V_{sample} \times t_0)$, where $V_{sample}=a \cdot b \cdot c$ and t_0 is the irradiation time. The boundary conditions read:

$$\left[\frac{\partial K_x}{\partial X} + \frac{h}{k}\cdot K_x\right]_{x=-\frac{a}{2}} = 0, \quad \left[\frac{\partial K_x}{\partial X} + \frac{h}{k}\cdot K_x\right]_{x=\frac{a}{2}} = 0 \quad (6.a)$$

$$\left[\frac{\partial K_y}{\partial Y} + \frac{h}{k}\cdot K_y\right]_{y=\frac{b}{2}} = 0, \quad \left[\frac{\partial K_y}{\partial Y} + \frac{h}{k}\cdot K_y\right]_{y=-\frac{b}{2}} = 0, \quad (6.b)$$

$$\left[\frac{\partial K_z}{\partial Z} - \frac{h}{k}\cdot K_z\right]_{z=0} = 0, \left[\frac{\partial K_z}{\partial Z} + \frac{h}{k}\cdot K_z\right]_{z=c} = 0, \quad (6.c)$$

Here, a, b and c are the geometrical dimensions of the sample, along X, Y and Z axes, h is the heat transfer coefficient, K_x, K_y, Kz stand for the Eigen-functions and α_i, β_j, χ_o are their corresponding Eigen-values, respectively.

The corresponding solution of the heat equation is [11, 12]:

$$\Delta T(x,y,z,t) = \sum_{i=1}^{\infty}\sum_{j=1}^{\infty}\sum_{o=1}^{\infty} I_1(\alpha_i,\beta_j,\chi_o)I_2(\alpha_i,\beta_j,\chi_o,t)K_x(\alpha_i,x)K_y(\beta_j,y)K_z(\chi_o,z),$$

$$(7)$$

where by definition:

$$I_1(\alpha_i,\beta_j,\chi_o) = \frac{1}{C_iC_jC_o}\int_{-\frac{a}{2}}^{\frac{a}{2}}\int_{-\frac{b}{2}}^{\frac{b}{2}} K(\alpha_i,x)K(\beta_j,y)\cdot P(x,y)\cdot dxdy\int_0^c K_o(\chi_o,z)(6.23 - 4.36\cdot z)dz,$$

$$I_2(\alpha_i,\beta_j,\chi_o,t) = \frac{1}{\alpha_i^2+\beta_j^2+\chi_o^2}[1 - e^{-\gamma_{ijo}^2 t} - (1-e^{-\gamma_{ijo}^2(t-t_o)})h(t-t_o)],\quad (8)$$

with

$$\gamma_{ijo}^2 = \gamma(\alpha_i^2+\beta_j^2+\chi_o^2).\quad (9)$$

Here $P(x,y)$ is the incident density power delivered by the radiation beam.
C_i, C_j, and Co are normalization constants. The Eigen-functions inferred for the heat equation (5) with boundary conditions (6a-c) have the following explicit expressions:

$$K_x(\alpha_i,x) = \cos(\alpha_i\cdot x) + (h/k\alpha_i)\cdot\sin(\alpha_i\cdot x),\quad (10.a)$$

$$K_y(\beta_j,y) = \cos(\beta_j\cdot y) + (h/k\beta_j)\sin(\beta_j\cdot y),\quad (10.b)$$

$$K_z(\chi_0,z) = \cos(\chi_0\cdot z) + (h/k\chi_0)\sin(\chi_0\cdot z).\quad (10.c)$$

We mention that the Eigen-values can be determined from the boundary equations:

$$2\cot(\alpha_i a) = \frac{\alpha_i k}{h} - \frac{h}{k\,\alpha_i},\quad (11.a)$$

$$2\cot(\beta_j b) = \frac{\beta_j k}{h} - \frac{h}{k\beta_j},\quad (11.b)$$

$$2\cot(\chi_0 c) = \frac{\chi_0 k}{h} - \frac{h}{k\,\chi_0}.\quad (11.c)$$

4. Simulations and conclusions

We give in Figs. 2 and 3 the thermal fields under laser and electron beam irradiation at the same continuous-wave power (500 W) after an exposure time of 20s. One observes that the thermal fields are almost identical in the two cases, despite the fact that Lambert Beer (α=10^{-1}cm^{-1}) and Katz and Penfolds absorption laws are quite different. This implies that the supposition regarding the similarity between laser and electron irradiation results [7-10] at relatively high incident powers is fully justified.
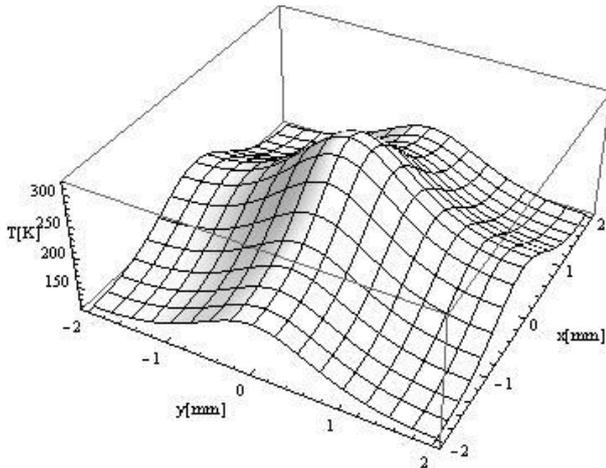
Fig. 2. Temperature field on graphite surface after 20s irradiation with an IR laser beam of 500W. In the following, T was used in the integral transform technique for the temperature variation rather than for absolute temperature
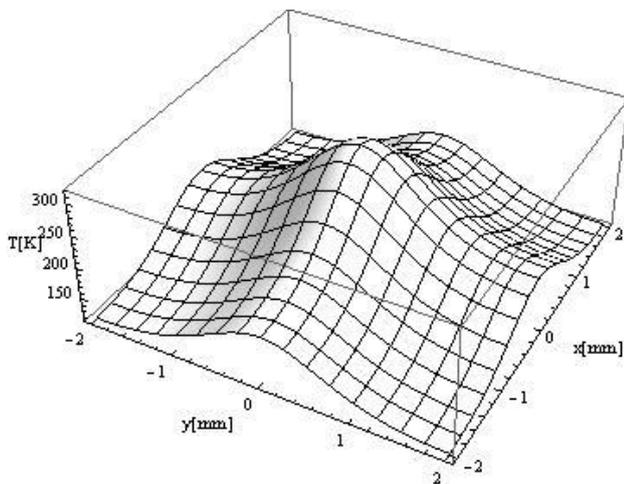

Fig. 3. Temperature field on graphite surface after 20 s electron beam irradiation at 500W and 6.5 MeV

References

[1] H. E. Cline, T. R. Anthony, J. Appl. Phys. **48**(9), 3895 (1977).
[2] M. Yamada, K. Nambu, K. Yamamoto, J. Appl. Phys. **57**(3), 965 (1985).
[3] A. M. Prokhorov, I. Ursu, V. I. Konov, I. N. Mihailescu, Philadelphia and New York, 275 (1990).
[4] C. W. White, P. S. Peercy, Academic Press, Inc. Published by Elsevier Inc. (1980).
[5] M. Sorescu, E. T. Knobbe, J. J. Martin, Journal of Materials Science **30**, 5944 (1995).
[6] Zhanbing Yang, Seiichi Watanabe, Takahiko Kato, Scientific Reports 3 (2013) Article number: 1201.
[7] L. Katz, A. S. Penfold, Rev. Mod. Phys. **24**(1), 28 (1952).
[8] M. Oane, D. Toader, N. Iacob, C. M. Ticoş, Nucl. Instr. Meth. Phys. Res. **318**, 232 (2014).
[9] M. Oane, A. Peled, R. Medianu, Notes on Laser Processing, Lambert Academic Publishing, Germany (2014).
[10] M. Oane, D. Ticoş, C. M. Ticoş, Charged Particle Beams Processing versus Laser Processing, Scholars' Press, Germany (2015).
[11] G. Popescu-Pelin, A. Bucă, M. Oane, L .Şufaru, I. N. Mihăilescu, Optoelectron. Adv. Mat. **9**(11-12), 1572 (2015).
[12] A. Bucă, V. Damian, M. Oane, R. V. Medianu, I. N. Mihăilescu, G. Popescu-Pelin, Optoelectron. Adv. Mat. **10**(1-2), 29 (2016).

_____
[*]Corresponding author: ion.mihailescu@inflpr.ro